

Micromanipulation of adhesion of phorbol 12-myristate-13-acetate-stimulated T lymphocytes to planar membranes containing intercellular adhesion molecule-1

Aydin Tözeren,* Linda H. Mackie,* Michael B. Lawrence,† Po-Ying Chan,† Michael L. Dustin,† and Timothy A. Springer†

*Department of Mechanical Engineering, The Catholic University of America, Washington, DC 20064; and

†The Department of Pathology, Harvard Medical School, Boston, Massachusetts 02115 USA

ABSTRACT This paper presents an analytical and experimental methodology to determine the physical strength of cell adhesion to a planar membrane containing one set of adhesion molecules. In particular, the T lymphocyte adhesion due to the interaction of the lymphocyte function associated molecule 1 on the surface of the cell, with its counter-receptor, intercellular adhesion molecule-1 (ICAM-1), on the planar membrane, was investigated. A micromanipulation method and mathematical analysis of cell deformation were used to determine (a) the area of conjugation between the cell and the substrate and (b) the energy that must be supplied to detach a unit area of the cell membrane from its substrate.

T lymphocytes stimulated with phorbol 12-myristate-13-acetate (PMA) conjugated strongly with the planar membrane containing purified ICAM-1. The T lymphocytes attached to the planar membrane deviated occasionally from their round configuration by extending pseudopods but without changing the size of the contact area. These adherent cells were dramatically deformed and then detached when pulled away from the planar membrane by a micropipette. Detachment occurred by a gradual decrease in the radius of the contact area. The physical strength of adhesion between a PMA-stimulated T lymphocyte and a planar membrane containing 1,000 ICAM-1 molecules/ μm^2 was comparable to the strength of adhesion between a cytotoxic T cell and its target cell. The comparison of the adhesive energy density, measured at constant cell shape, with the model predictions suggests that the physical strength of cell adhesion may increase significantly when the adhesion bonds in the contact area are immobilized by the actin cytoskeleton.

INTRODUCTION

Lymphocytes adhere transiently to a number of different cell types for normal migration between blood and other tissues (recirculation) and during generation of immune responses to foreign antigens. The molecular bridges that stabilize adhesion and define the duration of these encounters are formed by overlapping subsets of cell surface receptors and counter-receptors expressed on lymphocytes and diverse cell types. The T cell antigen receptor (TCR) recognizes foreign antigens bound to molecules of the major histocompatibility complex on other cells (Meuer et al., 1984). Other T cell adhesion receptors include lymphocyte function associated molecule 1 (LFA-1), which binds to its counter-receptors intercellular adhesion molecule (ICAM)-1 or ICAM-2, and CD2, which binds to LFA-3 on the surface of the target cell. T lymphocytes that have been stimulated to grow in culture show strong adhesion to non-antigen-bearing cells. This antigen-independent adhesion is mediated by CD2 LFA-3 and LFA-1 ICAM-1 interactions (Springer, 1990).

The interaction of an integrin adhesion receptor, LFA-1, with a member of the immunoglobulin superfamily, ICAM-1, is important in a large number of contexts. The ability of LFA-1 molecules, always present on the surface of lymphocytes, to bind ICAMs is regulated. Cross-linking of the TCR triggers a rapid (minutes) and transient (minutes) increase in binding of resting T lymphocytes to surfaces bearing purified ICAMs or to other cells (Dustin and Springer, 1989). An equally rapid but long-lasting (hours) increase in LFA-1 avidity for ICAMs can be triggered by treating T lymphocytes with phorbol 12-myristate-13-acetate (PMA), an activator of

protein kinase C (Dustin and Springer, 1989). The activation of protein kinase C also may lead to formation of pseudopods containing an increased concentration of F-actin in T lymphocytes (Phatak et al., 1988).

Double immunofluorescence studies indicate that the adhesion receptor LFA-1 may interact with cytoskeletal structures after the treatment of the cell with phorbol esters (Burn et al., 1988; Kupfer and Singer, 1989*a, b*). Talin, a protein molecule usually implicated to interact with actin, was found to remain uniformly distributed on cells that exhibited antibody-induced LFA-1 caps. If, however, the cells were treated with PMA before capping, talin codistributed with LFA-1 caps. The redistribution of talin did not occur upon capping membrane proteins unrelated to LFA-1 in the presence of PMA.

The micromanipulation of the adhering cell couples by suction pipettes may provide quantification of the forces required to detach cell couples (Evans and Leung, 1984; Sung et al., 1986; Tözeren et al., 1989). From micromanipulation data, a quantity related to the energy required to separate a unit area of adhering membranes, the adhesive energy density has been calculated for cell-cell adhesion mediated by multiple adhesion mechanisms (Evans and Leung, 1984; Tözeren et al., 1989).

We describe in Section 2 a micromanipulation technique used to determine the strength of adhesion between a cell and a planar membrane containing adhesion molecules (Tözeren et al., 1992). This method allows the characterization of the adhesive energy density contributed by the LFA-1/ICAM mechanisms at a known density of ICAM-1 in the planar membrane. In addition, the use of a single type of receptor in the planar

membrane enables one to avoid the complex topological features that may result due to the existence of bonds with different interaction lengths (Springer, 1990).

The predictions of an equilibrium model in which the cell adhesion is treated as a surface phenomena are presented next to set a scale for the adhesive energy density deduced from experimental data. The comparison of model predictions with our micromanipulation data suggests the possibility that cytoskeletal structures, anchored to LFA-1 integrin molecules, contribute to the strength of adhesion of activated T lymphocytes by resisting the peeling action of the cell membrane at the edge of conjugation.

METHODS

This study used a micromanipulation technique to quantify both the apparent contact area as well as the adhesive energy density between a T lymphocyte and a planar substrate containing one set of adhesion molecules (Tözeren et al., 1992). A glass-supported lipid bilayer containing ICAM-1 molecules was used as the planar substrate. The adhesion counter-receptor ICAM-1 was purified and reconstituted into egg liposomes by using the procedure described by Marlin and Springer (1987).

The glass chips ($2 \times 10 \times 0.1$ mm) supporting the lipid bilayer were cut from a grade-1 cover-slip (Fisher Scientific, Allied Corp., Pittsburgh, PA). These chips were coated with a planar membrane by adopting the method of McConnell et al. (1986). Briefly, the chips were boiled in a Linbro 7X detergent (ICN Flow Laboratories, Costa Mesa, CA) and water solution (1:6) for over 1 h. The chips were then rinsed in deionized water ~ 50 times over 1 h. Absolute ethanol was used in the last rinse, and the glass pieces were separated on filter paper to air dry. A glass chip was then positioned vertically in the chamber by using a flat glass chip as a back support. Both chips were glued with K-Fast super glue (Fisher Scientific) to the bottom of the chamber. A 5- μ l drop of liposome suspension was then placed on top of the glass chip, and the chamber was covered with moist towels to retard evaporation. After 25 min at room temperature (21–23°C), the cell chamber was flooded with the media [20 mM *N*-2-hydroxyethylpiperazine-*N'*-2-ethanesulfonic acid (Hepes), 0.14 M NaCl, 0.5 mM MgCl₂, 0.5 mM CaCl₂, 1 g/liter glucose, 0.1% bovine serum albumin, pH 7.4], and then the media was changed three times without exposing the planar membrane on the chip surface to air. As described in Lawrence and Springer (1991), the surface density of ICAM-1 in the upper leaflet of the planar bilayer was determined by using an immunoradiometric assay directly on the planar bilayers formed under identical conditions. The site density used in the experiments was $\cong 1,000/\mu\text{m}^2$ ($950 \pm 95/\mu\text{m}^2$).

The human T lymphocytes were purified as described by Dustin et al. (1989). Briefly, the resting T cells were isolated from whole blood by Ficoll-Hypaque centrifugation and nylon wool filtration. The micromanipulation data presented in the paper were obtained on three different dates, and each time the T cells were used within 24 h from the time the blood was drawn. The T cells were stored in a solution of RPMI/10% fetal calf serum (FCS)/25 mM Hepes (pH 7.4). Approximately 20 μ l of cell suspension at 5×10^6 cells/ μ l was added to the 1-ml cell chamber. In some experiments, 100 ng/ml PMA was added to the cell chamber.

The chamber was tilted slightly to allow cell sedimentation onto the membrane-coated glass chip. After 5 min of incubation, the cell chamber was placed on the microscope stage. To confirm the establishment of planar membrane with this procedure, we used liposomes made from a fluorescent phospholipid analogue (2 mol% NBD-phosphatidylethanolamine incorporated into egg phosphatidylcholine liposomes) for several control cases.

A micropipette mounted in a pneumatic micromanipulator (model SMM1-1; Technical Products International, Inc., St. Louis, MO) on the stage of the microscope was used to detach the T cells from the planar membrane. Micropipettes were made by pulling 0.7–1.0-mm-outer-diam pipettes (Thomas Scientific, Philadelphia, PA) on a pipette puller (PB-7; Narashige Scientific Laboratory, Tokyo, Japan). The pipettes were incubated with 100% FCS before micromanipulation to inhibit cell–pipette adhesion. The pressure inside the pipette was controlled by a manometer connected to the pipette by continuous water-filled tubing. Additional pressure was applied by mechanical syringe to the reservoir chamber. A pressure transducer (Validyne Engineering Corp., Northridge, CA), connected to the pipette by a continuous water connection, measured changes in pipette pressure.

The cells were observed with an inverted microscope equipped with two 15 \times eyepieces and a 10 \times eyepiece on the side port (Diaphot; Nikon Inc., Garden City, NY) and a 60 \times , 0.70-N.A.-long working distance objective (Nikon). The experiments were recorded on videotape with a video camera (Dage-MTI, Michigan City, IN) mounted on the side port. Time and pressure were displayed on the video monitor with a “data mixer” (Vista Electronics, La Mesa, CA). For data analysis, the tape was played through a video monitor equipped with a position analyzer (Vista Electronics) that provided a digital readout proportional to the distance between two sets of vertical and horizontal lines.

The micromanipulation procedure was initiated by focusing first on a lymphocyte adhering to the planar membrane. The cell was then captured by using a small aspiration pressure to hold part of the cell inside the pipette (50–100 dyn/cm²). The pressure in the pipette was increased incrementally to a level that would permit the complete detachment of the cell from the substrate as the pipette was pulled away gradually and/or kept at the same location. In each micropipette experiment, a different cell was detached from a different location of the planar membrane. The sequence of images from the television monitor was used to determine the geometric parameters needed for the quantification of the strength of cell adhesion. The experiments were carried out at room temperature (21–23°C).

DATA ANALYSIS

The geometric parameters determined from the videotape of the micromanipulation events are the radius of the pipette at its tip (R_p), the radius of conjugation (R_c), the maximal radial distance on the cell (R_m), the length of portion of the cell that remains between the pipette and the planar wall (L), and the angles that the unit vector normal to the cell surface makes with the direction of the pipette at the edge of conjugation and at the tip of the pipette (θ_c , θ_p). These parameters are identified in Fig. 1. Note that R_c , R_m , L , θ_c , and θ_p vary with time during the course of detachment.

In this study, the physical strength of adhesion between a T lymphocyte and a planar membrane containing ICAM-1 is characterized by determining the adhesive energy density between the cell and the substrate from micromanipulation data. The adhesive energy density (γ) is defined as the energy that must be supplied to detach a unit area of the cell membrane from the planar membrane. This parameter, frequently denoted as fracture energy density, is the energy per unit length absorbed at the moving boundary of separation. It has been used to describe nonequilibrium phenomena such as the propagation of a crack through a solid beam (Burrige and Keller, 1978). As noted by Gent (1982), some part of this energy is dissipated in deforming the interacting

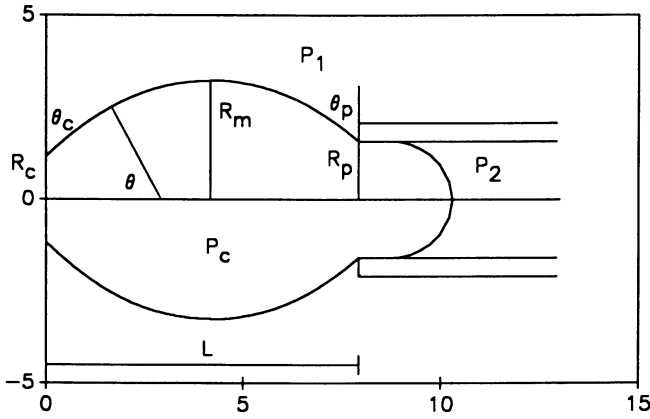


FIGURE 1 The schematic diagram of a cell being detached from the planar membrane by micromanipulation of the holding pipette.

surfaces. In engineering, the fracture energies are often found to depend on the speed of deformation and the test temperature, which are the properties characteristic of dissipative processes.

Lymphocyte model A

We shall consider in model A the case where the force exerted on the cell by the micropipette is transmitted to the contact line between the cell and the substrate by the meridional cell membrane tension. A typical T lymphocyte will be treated as an axisymmetric shell (cell membrane) encompassing a fluid-like substance (a highly viscous cell nucleus surrounded by less viscous cell cytoplasm). Leukocyte interior is a highly structured substance composed of various organelles, cytosol, and the fiber networks. Nevertheless, it flows readily into a micropipette during a suction experiment (Evans and Yeung, 1989). This liquidlike behavior of the cell interior may be due to the ease at which the connections between the structural elements of cell cytoskeleton break.

The cell membrane is defined here as the plasma membrane and the load bearing cytoskeletal structures that are attached to it, such as the actin-rich cortical layer. Although the content of filamentous actin (F-actin) in leukocytes increases significantly in response to PMA-stimulation or adhesion to a substrate, this increase is associated largely with the cell cortex attached to the plasma membrane (Southwick et al., 1989). The cell membrane bears large in-plane stresses (membrane tensions) but has negligible resistance to bending, except where there are sharp curvatures, such as at the contact line of the cell and the planar membrane.

For model A, the adhesive energy density γ can be expressed in terms of the contact angle θ_c and the meridional tension in the cell membrane at the edge of conjugation (T_c) as follows (Evans and Leung, 1984):

$$\gamma = T_c(1 - \cos \theta_c). \quad (1)$$

No experimental method exists to quantify the meridional tension at the edge of conjugation (T_c), but T_c can be evaluated analytically for the two cell membrane models considered below.

In model A1, the circumferential tension in the cell membrane (T_ϕ) is assumed negligible in comparison with the meridional membrane tension (T_s). As the cell is stretched in the direction of the pipette, actin fibers within the cortical shell may tend to align themselves along the meridional direction, resulting in an increased meridional tension.

In model A2, the tension in the cell membrane is assumed isotropic (the circumferential tension equals meridional tension). This model is valid for investigating the adhesion of lipid-bilayer capsules to various substrates. It may also be an appropriate model for a cell that does not deviate significantly from its round configuration during forced detachment.

In the following, we consider the phase of the cell detachment in which the deformed cell sustains the tensile force exerted by the micropipette without additional change in cell shape. Under these conditions, the pressure distribution inside the cell is expected to be uniform. Hence, the equations of static equilibrium for an axisymmetric membrane shell under constant pressure (Timoshenko, 1940) can be used to obtain the cell membrane tension at the edge of conjugation.

For model A1, the meridional tension T_c is given by the following equation:

$$T_c = (P_c - P_2)(R_p^2)/(2R_c), \quad (2a)$$

where P_c is the pressure in the cell and P_2 is the pressure in the pipette. The suction pressure determined in the experiments is equal to the pressure in the micromanipulation chamber (P_1) minus the pressure in the pipette (P_2).

Again, using the equations of static equilibrium for the cell membrane and assuming that the contact angle $\theta = \theta_p$ at $R = R_p$ and $\theta = \theta_c$ at $R = R_c$, the following relation is obtained for $(P_c - P_2)$:

$$1 - [(P_1 - P_2)/(P_c - P_2)] = (\sin \theta_p - \sin \theta_c)/[1 - (R_c/R_p)^2]. \quad (2b)$$

For model A2, the membrane tension at the edge of conjugation (T_c) can be expressed as:

$$T_c = (P_c - P_2)(R_p)/2. \quad (3a)$$

Similarly, the pressure difference $(P_c - P_2)$ can be written for model A2 a:

$$1 - [(P_1 - P_2)/(P_c - P_2)] = (\sin \theta_p - (R_c/R_p) \sin \theta_c)/[1 - (R_c/R_p)^2]. \quad (3b)$$

The adhesive energy density (γ) computed by using model A2 is consistently higher than the corresponding value obtained by using model A1.

Tözeren et al. (1989) computed the adhesive energy density between a cytotoxic T cell and its target cell by using the following equation:

$$\gamma = (P_1 - P_2)[R_p^2/(2R_c)](1 - \cos \theta_c)/(\sin \theta_p/\sin \theta_c). \quad (4)$$

In deriving Eq. 4, the pressure difference between the cell and the surrounding medium was assumed equal to 0 (Evans and Leung, 1984). As a result of this assumption, the condition of local force balance in the direction normal to the cell membrane (Laplace's Law) cannot be satisfied exactly. The results presented in the next section indicate, however, that the adhesion parameter γ computed from micromanipulation data by using Eq. 4 is similar in value to the corresponding estimate obtained by using model A1.

Lymphocyte model B

Consider next a leukocyte model in the form of a viscoelastic sphere of radius R_0 . Although leukocytes are not spheres with homogeneous material properties, nevertheless, elastic energy may be stored in the actin-rich cell cytoskeleton as the cell spreads on the substrate.

The adhesive energy density for a viscoelastic sphere freely interacting with a planar substrate is given by the following equation:

$$\gamma = GR_0^3/(9R_0^2), \quad (5a)$$

where G (dyn/cm²) is the long term elasticity coefficient of the sphere (Johnson, 1985). An estimate of the stiffness parameter G can be obtained by using small aspiration tests on leukocytes (Sung et al., 1988). Eq. 5a shows that adhesive energy density is proportional to the third power of the steady-state radius of contact measured in micromanipulation experiments.

The application of a tensile force on the solid sphere in contact with the planar wall causes the contact area to shrink toward 0. In the case of micromanipulation experiments, this tensile force can be represented by the suction pressure multiplied by the cross-sectional area of the tip of the micropipette (PR_p^2). When the pipette force reaches a critical value equal to $(3\pi\gamma R_0)$, the situation becomes unstable and the surfaces separate (Johnson, 1985). The critical condition of detachment for model B is then given by the following equation:

$$\gamma = PR_p^2/(3R_0). \quad (5b)$$

The elastic energy stored in the sphere during its free interaction with the planar substrate is spent in propagation of a crack through the contact area.

RESULTS

We carried out a set of micromanipulation experiments to investigate the physical strength of adhesion between

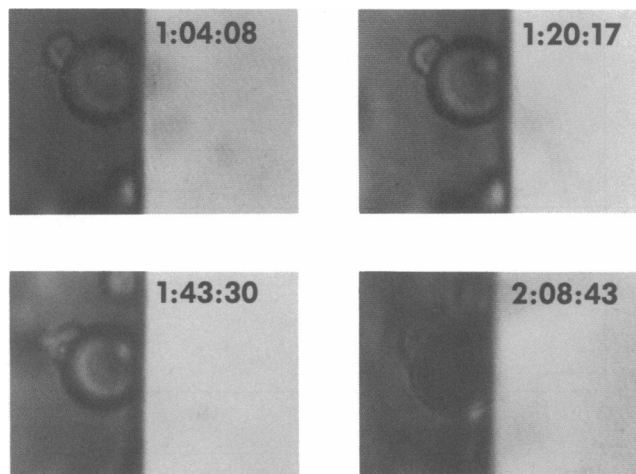


FIGURE 2 Sequence of photographs showing the contour of a PMA-stimulated T lymphocyte freely interacting with a planar membrane reconstituted with 1,000 ICAM-1 molecules/ μm^2 . The numbers on top of the photographs represent, in order, hours, minutes, and seconds.

a PMA-stimulated T lymphocyte and a planar membrane containing 1,000 transmembrane ICAM-1 molecules/ μm^2 . The data obtained with fluorescence recovery after photobleaching technique indicate that the transmembrane macromolecules are transversely immobile within the plane of a glass-supported lipid bilayer (Brian and McConnell, 1984; Watts et al., 1984; McConnell et al., 1986; Chan et al., 1991). The immobilization of transmembrane molecules in the planar membrane is probably due to interaction of the cytoplasmic domain with the glass surface.

The resting T lymphocytes did not stick to clean glass suspended in the medium or to the planar membrane with or without ICAM-1 when the cells were kept in contact with the planar substrate for 5–10 min. The activation of T lymphocytes by the addition of the 100 ng/ml PMA into the suspending media induced strong cell adhesion to the vertical glass-supported planar membrane containing ICAM-1 but not to the planar membrane without ICAM-1. Small suction pressures (100–400 dyn/cm²) were needed to pick a cell from the bottom of the glass chamber by using a micropipette.

Morphology of PMA-stimulated T cells adhering to a planar membrane containing ICAM-1

We investigated the effect of the period of incubation on the contour of PMA-stimulated T lymphocytes in contact with a planar membrane reconstituted with 1,000 ICAM-1 molecules/ μm^2 . The time sequence of cell contours obtained with this procedure for a typical cell is shown in Fig. 2. The contact angle, θ_c , and the radius of conjugation, R_c , remained fairly constant during a 2-h period, with only a slight decrease measured. We ob-

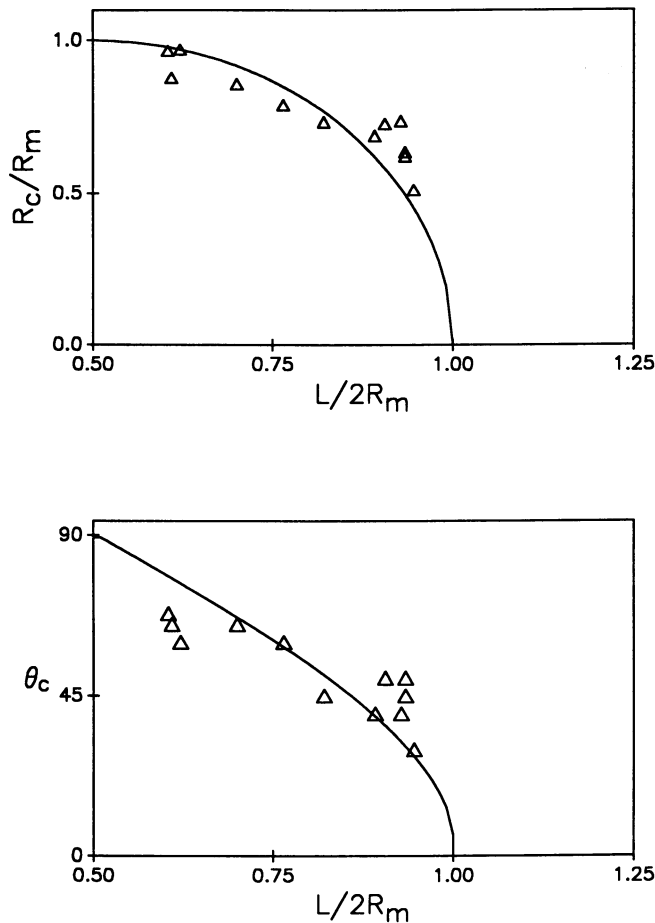


FIGURE 3 Comparison of experimental data on the morphology of T lymphocytes adhering to a planar membrane containing $1,000 \text{ ICAM-1}/\mu\text{m}^2$ with the corresponding prediction of the cortical shell-liquid core model (Evans and Yeung, 1989). Geometric parameters were measured after 10 min incubation but before micromanipulation (R_c , radius of conjugation; θ_c , the contact area at the edge of conjugation; R_m , maximum radial distance along the axisymmetric cell surface; L , the maximum dimension of the cell in the direction normal to the planar bilayer). The discrete points represent experimental data. Continuous lines are the model predictions.

served similar behavior for all the cells videotaped for extended periods of free conjugation.

It is not possible to produce cell contours for cell-substrate interaction before micromanipulation by using the equations of model A1. This indicates that the unidirectional tension (meridional tension) is not a good approximation for the cell membrane tension distribution before micromanipulation.

Model A2, on the other hand, predicts that the contours of cells attached to a planar substrate must be spherical in form. This is also the prediction of the cortical shell-liquid core model of leukocytes put forward by Evans and Yeung (1989). To test the validity of this prediction, we plotted in Fig. 3 the ratio R_c/R_m (*top*) and the contact angle θ_c (*bottom*) as a function of the dimensionless cell length (L/R_m). The discrete points identify

the experimental data, whereas continuous lines represent the predictions of model 2. Fig. 3 shows that the morphology of T cells before forced detachment is consistent with the cortical shell-liquid drop model of leukocytes.

The morphology of T cells adhering to planar membranes reconstituted with ICAM-1 molecules is also consistent with the prediction of model B, obtained by using small strain analysis (Johnson, 1985). Large deformation analysis of a homogeneous spherical particle that is brought into contact with a planar substrate is not yet available in the literature.

The T cells attached to the planar membrane deviated occasionally from their round configurations by extending projections (Fig. 4). Similar to the pseudopod projection history of granulocytes (Schmid-Schönbein, 1990), the active process of extension of a projection and its subsequent retraction lasted typically $\sim 1\text{--}2$ min. The apparent contact area did not change during active cell movement.

The contact areas of T cells adhering to a planar bilayer containing $1,000 \text{ ICAM-1}/\mu\text{m}^2$ is significantly greater than that of Jurkat T cells (which have high expression of CD2 receptors) interacting with a glass-supported lipid bilayer that was reconstituted with transmembrane LFA-3 molecules at the same site density (Tözeren et al., 1992). Jurkat T cells did not spread on planar membranes containing $1,000$ transmembrane LFA-3/ μm^2 , but each cell formed a point contact with the planar substrate.

The parameters of Jurkat cell deformability, assessed by micropipette aspiration, are similar to that of other leukocytes (Tözeren et al., 1992). Both models A and B predict that when a cell interacts with two different planar substrates, the cell-substrate interaction that results in a larger contact area corresponds to the one with greater adhesive energy density. Adhesion molecules CD2 and LFA-3 are members of the immunoglobulin superfamily. In contrast to LFA-1-ICAM-1 interaction, these receptors mediate cell adhesion in the absence of Mg^{2+} and at low temperatures (4°C), whereas the cytoskeletal interference with adhesion must be minimal (Springer, 1990). Hence, the active participation of cell cytoskeleton may be a reason for the physical strength of the integrin-mediated cell adhesion investigated here.

Forced detachment of PMA-stimulated T lymphocytes from planar bilayers containing ICAM-1 molecules

We conducted a set of micromanipulation experiments to investigate the physical strength of adhesion between a PMA-stimulated T lymphocyte and a planar membrane reconstituted with $1,000 \text{ ICAM-1}/\mu\text{m}^2$. The results of nine micromanipulation experiments are reported in Table 1. In these experiments, the cells remained symmetric during detachment as judged from the side view. The geometric parameters R_c , R_p , θ_c , and

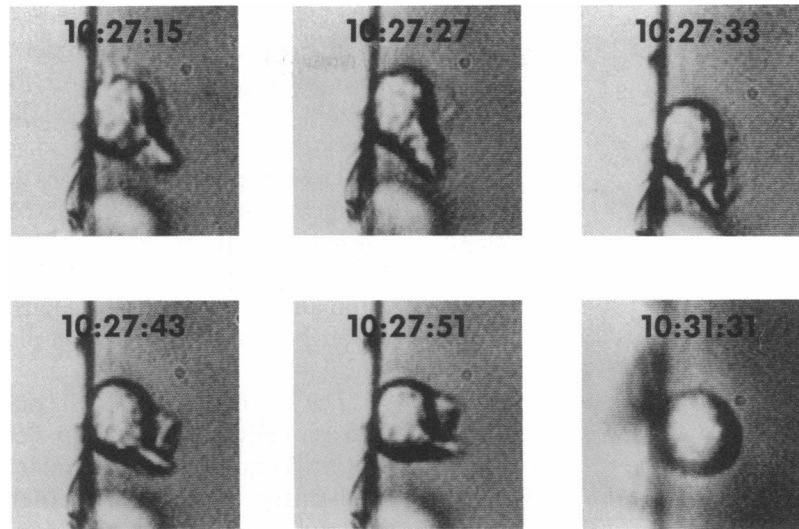


FIGURE 4 Sequence of photographs recording the active movement of a PMA-stimulated T lymphocyte in contact with a planar membrane containing $1,000 \text{ ICAM-1}/\mu\text{m}^2$. The numbers on top of the photographs represent, in order, hours, minutes, and seconds.

θ_p could be determined from the videotapes of the micromanipulation events. Table 1 indicates that the micromanipulation data evidenced variation from cell to cell, similar to the data reported by Sung et al. (1986). This variation may reflect the heterogeneity of the T cell population in either their capacity to respond to PMA or their LFA-1 expression level. A subpopulation of T lymphocytes, known as memory cells, have higher LFA-1 expression than the rest of the T cell population (Sanders et al., 1988). In our experiments, we have not differentiated between the subpopulations of T lymphocytes because our goals were to establish the order of magnitude of the forces required to detach a T cell from the ICAM-1 containing planar membrane and to characterize the cell deformation before micromanipulated detachment.

The micromechanism of cell detachment from the membrane-coated glass chip is not known. It is possible

that part of the cell membrane might have been sheared off the cell and remained behind on the planar surface while the cell quickly sealed itself. The cell detachment might also have occurred by the detachment of LFA-1 receptors from their counter-receptors ICAM-1 and by the extraction of LFA-1-ICAM-1 bonds from either the cell membrane or the planar bilayer.

Fig. 5 presents a typical sequence of micromanipulation events depicting the time course of detachment of a PMA-stimulated T lymphocyte from the planar substrate reconstituted with ICAM-1 molecules. Fig. 5 indicates that the cell undergoes a significant deformation before it detaches from the lipid-bilayer-coated glass chip and that the cell detachment occurs by the gradual reduction of the radius of conjugation.

Fig. 5 also indicates that the deformed T cell can sustain the force exerted by the pipette for ≥ 4 s without additional change in cell morphology (see frames identified with 10:50:23, 10:50:26, and 10:50:27 in Fig. 5). Because viscous stresses in the cell membrane and the cytoplasm are equal to 0 when the local rate of deformation is equal to 0, the uniform cell pressure is expected to be a good approximation for this phase of the cell detachment.

In Fig. 6, we plotted the radii of the contact areas between the T lymphocytes and the planar membrane as a function of time during the course of separation for three typical micromanipulation experiments. The rate of peeling (dR_c/dt) was not prescribed a priori but determined later from the videotapes of the micromanipulation events. The control of peeling rate is no easy task, because the direction in which the radius of conjugation decreases is perpendicular to the axis of the pipette used to detach the cell from the substrate. Nonetheless, Fig. 6 shows that the peeling of the cell is typically slow at first but accelerates at the final stages of cell detachment.

TABLE 1 Micromanipulation data for the detachment of a PMA-stimulated T lymphocyte from a planar membrane reconstituted with $1,000 \text{ ICAM-1}/\mu\text{m}^2$

Experiment	R_p	θ_c^0 * ($^\circ$)	R_m^0 *	R_c^0	$(P_1 - P_2)^{\ddagger}$
	μm		μm	μm	10^3 dyn/cm^2
1	1.4	55	5.4	3.75	3.2
2	2.2	55	4.7	3.4	0.9
3	2.2	68	4.2	3.9	2.9
4	2.2	50	4.9	3.1	3.9
5	2.2	65	5.6	4.6	3.7
6	2.2	68	4.9	3.4	1.9
7	2.2	45	4.3	3.3	4.1
8	2.2	45	5.2	1.75	1.4
9	2.2	60	4.7	3.2	6.8

* The superscript 0 identifies the values of the parameters before the initiation of cell detachment. $\ddagger(P_1 - P_2)$ denotes the suction pressure used to detach the cell from the planar membrane.

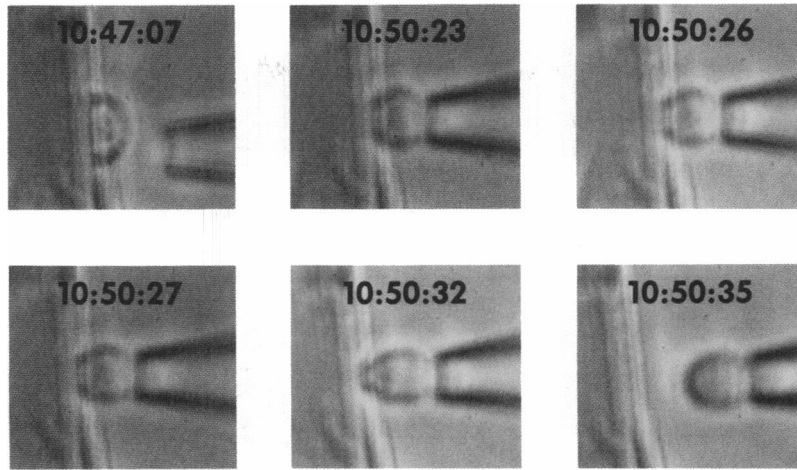


FIGURE 5 Sequence of photographs showing the time course of detachment of a PMA-stimulated T lymphocyte from a planar membrane reconstituted with 1,000 ICAM-1 molecules/ μm^2 . The numbers on top of the photographs represent, in order, hours, minutes, and seconds.

The adhesive energy density (γ) versus radius of conjugation (R_c) is shown in Fig. 7 for three different micromanipulation experiments discussed in Fig. 6. The adhesion parameter γ is ≈ 0.1 dyn/cm when evaluated with model A1 and ≈ 0.2 dyn/cm when evaluated by model A2 for the T cell shown in Fig. 5 at the instances the cell shape remained constant (triangular symbols in the figure). Fig. 7 shows that both the upper and the lower estimates of the adhesion parameter γ increases during the course of the detachment of a T cell from an ICAM-1-enriched planar membrane. Because the bonds linking the cell to the planar membrane are likely to be laterally fixed, the increase in these estimates of γ cannot be attributed to bond migration during disaggregation, as was proposed for T cell target cell interaction (Tözeren et al., 1989). It is possible that this increase reflects not necessarily an increase in the actual adhesive energy density but an increase in the energy required to bend the cell membrane as the contact area diminishes toward 0.

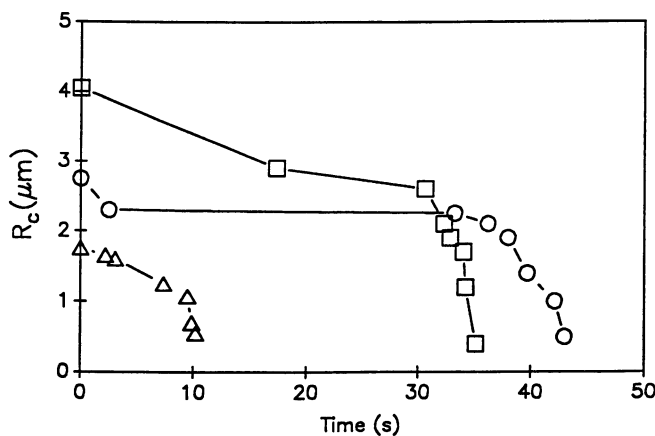


FIGURE 6 Time history of the radius of conjugation during detachment of the T lymphocytes from the ICAM-1 containing membrane for three typical micromanipulation experiments.

Shown in Fig. 8 are the experimentally determined cell contours (column 1) and the corresponding cell contours computed by using equations for model A1 (column 2) and model A2 (column 3). The cell contour determined by model A2 deviates from the experimental

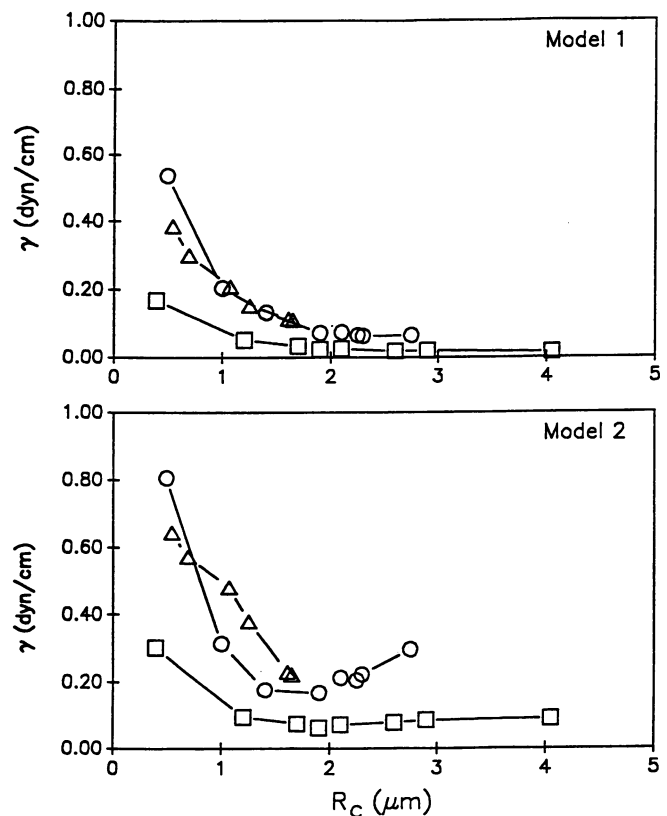


FIGURE 7 Adhesion energy density versus contact radius. The upper and lower estimates of the adhesive energy γ between PMA-stimulated T lymphocytes and a planar membrane containing ICAM-1 as a function of the radius of conjugation for the three experiments discussed in Fig. 6. The symbols used to identify the cells are the same as in Fig. 6.

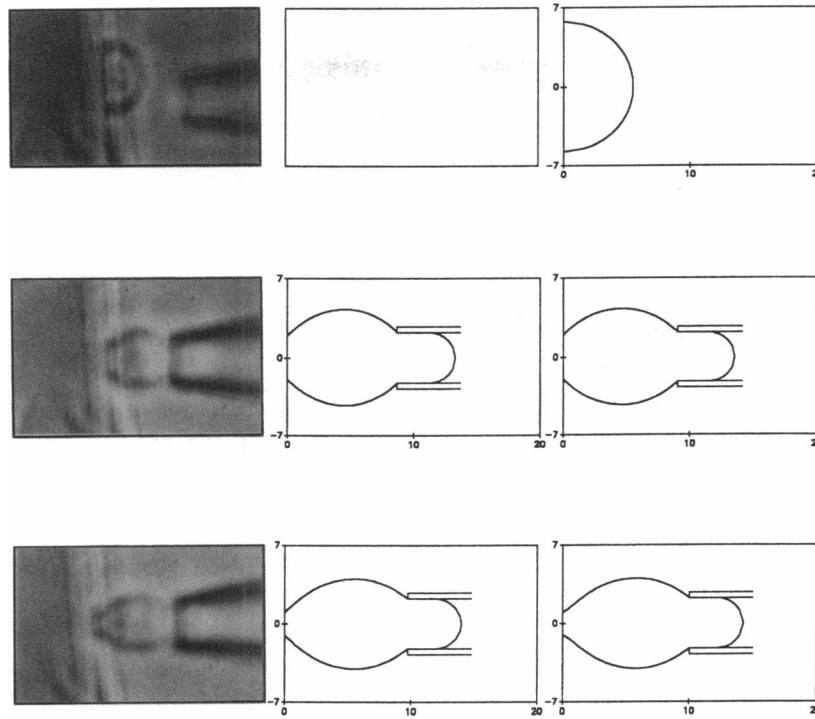


FIGURE 8 The modeled detachment of a PMA-stimulated human T lymphocyte from a planar membrane containing ICAM-1. Column 1 shows the actual micromanipulation events. Columns 2 and 3 show the corresponding cell contours computed for models 1 and 2, respectively. Only the part of the cell contour that remains between the planar membrane and the tip of the pipette was computed. The cell projection inside the pipette was schematically drawn. The data used in the computations are as follows: row 1, $R_c = 3.8 \mu\text{m}$ and $R_m = 4.1 \mu\text{m}$; row 2, $R_p = 2.1 \mu\text{m}$, $R_c = 1.9 \mu\text{m}$, $R_m = 4.1 \mu\text{m}$, and $\theta_p = 45^\circ$; row 3, $R_c = 1.0 \mu\text{m}$, $R_m = 3.85 \mu\text{m}$, and $\theta_p = 50^\circ$.

observation at later stages of cell detachment (Fig. 8, row 3). In contrast with the experimental observation, model A2 predicts a change in the sign of the meridional cell surface curvature in the region close to the planar membrane.

The adhesive energy density predicted by model B for the T-cell-ICAM-1 interaction can be computed from micromanipulation data by using Eq. 5b. The adhesion parameter $\gamma = 0.15 \pm 0.05 \text{ dyn/cm}$ when the mean T lymphocyte radius is taken to be equal to $3.5 \mu\text{m}$. This value is comparable with the predictions of model A for the initial phase of the forced cell detachment. On the other hand, consistent with the evaluations obtained from the morphology of the adhering cells, it is two orders of magnitude greater than that evaluated for Jurkat cell-transmembrane LFA-3 interaction at the same site density (Tözeren et al., 1992).

Adherence strength of cytotoxic T cells to their target cells

The adhesive energy density γ between a cytotoxic T cell and its target cell, computed from the micromanipulation data (Sung et al., 1986) by using Eq. 4, is $\sim 0.1\text{--}0.2 \text{ dyn/cm}$ at the initiation of cell detachment and increases approximately by a factor of 10 during the course of cell detachment (Tözeren et al., 1989). We reinvestigated this case by using the equations of models A1 and

A2. The photographs, presented by Sung et al. (1986), illustrating the time course of detachment of a cytotoxic T cell from its target cell, have been reproduced in column 1 of Fig. 9. Also shown in Fig. 9 are the corresponding cell contours computed for model A1 (column 2) and model A2 (column 3). The cell contours predicted by model A1 are better representations of the actual cell contours in cases where the cell elongates extensively along the direction of the pipette.

The γ values predicted by model A1 are within 5% of the γ values obtained by using Eq. 4, which neglects the pressure difference between the cell interior and the surrounding media. The γ values computed for rows 1–3 in Fig. 2 by using model A1 are, respectively, 0.1, 0.2, and 0.5 dyn/cm. The corresponding values for model A2 are 0.2, 0.3, and 0.8 dyn/cm. These values are comparable to the corresponding γ values shown in Fig. 7 for the interaction of PMA-stimulated T lymphocytes with planar membranes containing transmembrane ICAM-1, suggesting that the T cell adhesion mediated by LFA-1-ICAM-1 interaction has similar physical properties to that of T cell-target cell interaction.

Adherence strength predicted by an equilibrium model

The investigation of the micromechanics of adhesion at equilibrium is important for the purpose of setting a

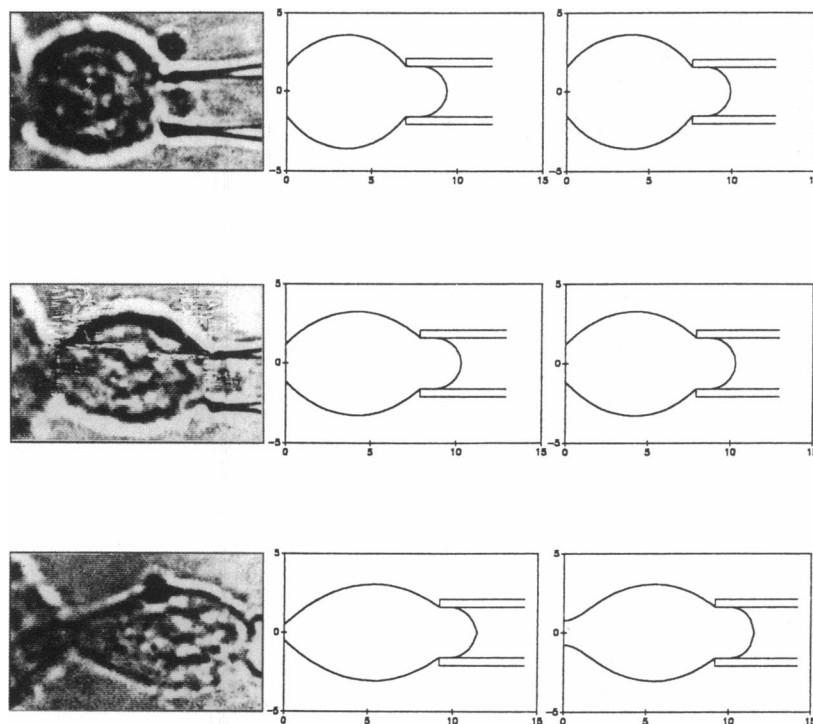


FIGURE 9 The detachment by micromanipulation of a cytotoxic T cell from its target cell. The photographs in rows 1, 2, and 3 of column 1 correspond, respectively, to Fig. 1, B–D, of Tözere et al. (1989). These photographs were obtained by Sung et al. (1986) and illustrate the time sequence of the T cell peeling from its target cell. The corresponding cell contours computed for models 1 and 2 are shown in columns 2 and 3, respectively. Only the part of the cell contour that remains between the planar membrane and the tip of the pipette was computed. The cell projection inside the pipette was schematically drawn. The experimental data used in the computations are as follows: row 1, $R_p = 1.2 \mu\text{m}$, $R_c = 1.6 \mu\text{m}$, $R_m = 3.6 \mu\text{m}$, and $\theta_p = 37^\circ$; row 2, $R_c = 1.2 \mu\text{m}$, $R_m = 3.3 \mu\text{m}$, and $\theta_p = 47^\circ$; row 3, $R_c = 0.5 \mu\text{m}$, $R_m = 3.0 \mu\text{m}$, and $\theta_p = 53^\circ$.

scale for the adhesive energy density γ , used here as a measure of the physical strength of adhesion.

The cell adhesion model presented by Bell et al. (1984) for equilibrium conditions formulates the cell-substrate adhesion as a surface phenomena. The specific cell adhesion is assumed to be due to the reversible interaction of a set of laterally mobile receptors on the cell surface with their similarly mobile counter-receptors on the planar membrane. The adhesion of the cell to the substrate is opposed by the nonspecific repulsion and the cell membrane tension acting at the edge of conjugation.

In the case where the membrane tension plays a negligible role in limiting the conjugation area, the model predicts that the nonspecific repulsive energy density Ω is proportional to the surface density of the bonds (n), constant of proportionality being the Boltzmann constant, k_b , multiplied by the absolute temperature T ($\Omega = k_b T n$, where $k_b T = 4.1 \times 10^{-14}$ dyn/cm at 25°C). Similarly, Tözere et al. (1989) showed that the adhesive energy density (γ), defined by Eq. 1, is equal to $k_b T n$, provided that the nonspecific repulsive energy density (Ω) between the cell and the substrate is negligible. Using the procedure outlined in Tözere (1990), it is not difficult to show that in the more general case, the sum of the nonspecific repulsive energy density (Ω) and the adhesive energy density (γ) is equal to $k_b T n$:

$$\gamma + \Omega = k_b T n. \quad (6a)$$

According to Eq. 6a, the maximum value of γ predicted by the equilibrium model is equal to 0.004 dyn/cm ($k_b T n = 0.004$ dyn/cm, $n = 1,000/\mu\text{m}^2$). In the micromanipulation experiments reported here, however, the adhesion parameter γ was found to be 0.1 – 0.2 dyn/cm at constant cell shape. This discrepancy may be due to the fact that in the system considered here, the LFA-1 ICAM-1 bonds are not laterally mobile as assumed in the model but are immobilized in the contact area between the cell and the substrate. If one again assumes a bimolecular interaction between LFA-1 and the laterally immobile ICAM-1, adhesion parameter γ must satisfy the following relation:

$$\gamma + \Omega = 2k_b T m_o \ln [1 + n/(m_o - n)], \quad (6b)$$

where m_o is the surface density of the ICAM-1 molecules ($1,000$ sites/ μm^2). Eq. 6b can predict values comparable to the experimental finding, when the surface density of adhesion bonds approaches the corresponding density of ICAM-1 molecules embedded in the planar membrane. The reason for this is that the surface density of immobile adhesion bonds (and the force generated by them) decays less with increasing bond strain than that for mobile bonds. An implication of this prediction is that in T

cell-target cell interaction, cytoskeletal structures that are anchored to LFA-1 molecules may provide additional strength to LFA-1 ICAM-1 bonds by making these bonds immobile in the contact region (Burrige et al., 1988). It would be of interest to pursue this mechanism further in models and in experiments.

It is also possible that the surface density of adhesion bonds may be far from equilibrium distribution even at constant cell shape. This type of behavior is observed, for example, in the mechanical response of active skeletal muscle fibers to step changes in fiber length. In cell-cell interaction, adhesion bonds may become stronger when stretched, as proposed by Dembo et al. (1988), and the cell peeling by micromanipulation occurs not by bond breakage, as assumed in the model, but by extraction of LFA-1 or ICAM-1 either from the cell membrane or from the planar membrane.

Effect of the cell content viscosity on the membrane tension at the edge of conjugation

At finite rates of cell deformation, the pressure distribution in the cell may depend strongly on the viscosity of the cell content. The viscosity of the leukocyte cytoplasm has been assessed by aspirating a small portion of the cell inside a micropipette. The viscous coefficient of the cytoplasm deduced with this procedure is ≈ 35 dyn-s/cm² for human Jurkat T cells (Tözeren et al., 1992) and 300 dyn-s/cm² for more typical leukocytes (Dong et al., 1988).

Using whole cell suction experiments, Evans and Yeung (1989) evaluated the effective viscosity of the interior of granulocytes to be $\sim 2,000$ dyn-s/cm². This value was obtained by comparing the experimental data with the computational predictions of Yeung and Evans (1989). In this process, the value of the cell membrane viscosity (η) was varied in a restricted range, whereas the cell content viscosity (μ) was kept approximately constant at a value that gives the best fit to data for $\eta \cong 0$. The data of Evans and Yeung (1989) can also be represented reasonably well with the predictions of Yeung and Evans (1989), valid for arbitrary values of η , provided that the value of μ is reduced from 2,000 dyn-s/cm² to a value determined by curve fitting data. The scatter in the micromanipulation data does not allow one to eliminate cell models with finite cell membrane viscosity.

Another reason this high viscosity value is not applicable to T cells is the inherent structural differences between the two leukocyte types. The number of granules within the cytoplasm of a T cell (45) is much less than for other leukocytes (4,500 for neutrophils and 2,000 for monocytes) (Schmid-Schönbein, 1990). The contribution of the cell nucleus to the effective viscosity may be

negligible in small aspiration tests but significant in experiments where the entire cell is sucked into the pipette.

To investigate the effect of the rate of cell elongation on the T cell membrane tension, we considered a simple structural model for T lymphocytes in which the cell nucleus is represented as a rigid sphere of radius R_n and the cytoplasm as a fluid with viscosity μ . The modeled cell takes the form of a sphere with radius R_o in suspension. The parameters R_o (3.5 μm) and R_n (2.3 μm) were chosen in accordance with the typical dimensions of lymphocytes, given in Table 1 of Schmid-Schönbein (1990). During the micromanipulation procedure, the outer shell of the modeled cell was assumed to form an ellipsoid whose dimensions change with time in such a way that its volume remains constant.

The lubrication analysis of cytoplasmic flow within the model cell shows that the T lymphocytes can elongate significantly in response to the pipette force, even without a significant change in the shape of the cell nucleus. To accommodate the stretching action of the pipette pulling the cell away from the planar substrate, the cytoplasm squeezes from the central region around the nucleus to the ends of the elongated cell. This flow results in an increase in pressure around the nucleus. The maximum pressure occurs at the cross-section corresponding to the maximum cell diameter.

We computed next the meridional cell membrane tension at the edge of conjugation for the nonuniform cell pressure distribution discussed above. The results indicated that T_c , and therefore $\gamma = T_c(1 - \cos \theta_c)$, increases by $\sim 30\%$ when cell content viscosity is taken equal 2,000 dyn-s/cm² as opposed to 0 and the rate of cell deformation is set equal to the experimentally observed value [$(dL/dt)/L < 0.05 \text{ s}^{-1}$]. Hence, the computation of the adhesion parameter γ from micromanipulation data with the procedure outlined in Data analysis is expected to be valid for the rates of cell peeling observed in our experiments.

DISCUSSION

In this study, we investigated the biophysical parameters of T lymphocyte adhesion mediated by the interaction of the adhesion receptors LFA-1 on the surface of the T lymphocyte with ICAM-1 counter-receptors on the surface of the planar membrane.

Our experiments showed that resting T lymphocytes did not adhere to planar membranes reconstituted with ICAM-1 receptors. These cells interacted strongly with the same substrate after PMA stimulation. The radius of the contact area between a PMA-stimulated T lymphocyte and a planar membrane containing 1,000 ICAM-1 molecules/ μm^2 increased within the first 10 min of incubation and remained constant or decreased slightly over the next few hours. The contact area did not change even during active cell movement (extension and subsequent

retraction of a pseudopod). The contact area measurements presented here are in agreement with the large areas of close membrane opposition between T lymphocytes and antigen-bearing cells determined by using other techniques (Kalina and Berke, 1976; Sanders et al., 1986).

T lymphocytes deformed significantly during the course of detachment from the planar membrane containing 1,000 transmembrane ICAM-1 molecules/ μm^2 . The cell detachment occurred by the gradual reduction of the contact area. The extent of T-lymphocyte deformation was comparable with the corresponding deformation, reported by Sung et al. (1986), of a cytotoxic T cell while it was being detached from its antigen-presenting cell at comparable rates. In contrast, Jurkat T cells detached from a planar membrane containing 1,000 transmembrane LFA-3 rapidly and without a significant change in cell morphology (Tözere et al., 1992).

The adhesive energy density between a T lymphocyte stimulated with PMA and a planar membrane reconstituted with 1,000 ICAM-1 molecules/ μm^2 was ~ 0.1 – 0.2 dyn/cm at the initiation of detachment. The physical strength of adhesion was comparable in magnitude to the corresponding strength of adhesion between a cytotoxic T cell and its target cell.

The comparison of the adhesion parameter γ determined from micromanipulation data with the prediction of a biophysical model (Tözere, 1990) suggests a mechanism in which the metabolically driven cytoskeletal structures, anchored to LFA-1 integrin molecules, augment the strength of cell adhesion by resisting the peeling action of the cell membrane.

We thank Doctor Richard Skalak for useful discussions on cell adhesion.

This research was supported by National Institutes of Health grants CA-31798 and GM-41460 and National Science Foundation grants BCS-8906330 and BCS-8908508.

Received for publication 9 January 1991 and in final form 11 October 1991.

REFERENCES

- Bell, G. I., M. Dembo, and P. Bongrand. 1984. Cell-cell adhesion: competition between nonspecific repulsion and specific bonding. *Biophys. J.* 45:1051–1064.
- Brian, A. A., and H. M. McConnell. 1984. Allogenic stimulation of cytotoxic T cells by supported planar membrane. *Proc. Natl. Acad. Sci. USA.* 81:6159–6163.
- Burn, P., A. Kupfer, and S. J. Singer. 1988. Dynamic membrane-cytoskeletal interactions; specific association of integrin and talin arises in vivo after phorbol ester treatment of peripheral blood lymphocytes. *Proc. Natl. Acad. Sci. USA.* 85:497–501.
- Burridge, K., K. Fath, T. Kelly, G. Nuckolls, and C. Turner. 1988. Focal adhesions: transmembrane junctions between the extracellular matrix and the cytoskeleton. *Annu. Rev. Cell Biol.* 4:487–525.
- Burridge, R., and J. B. Keller. 1978. Peeling, slipping and cracking: some one dimensional free-boundary problems in mechanics. *SIAM Rev.* 20:31–61.
- Chan, P. Y., M. B. Lawrence, M. L. Dustin, L. Ferguson, D. Golan, and T. A. Springer. 1991. The influence of receptor lateral mobility on adhesion strengthening between membranes containing LFA-3 and CD2. *J. Cell Biol.* 115:245–256.
- Dembo, M., D. C. Torney, K. Saxman, and D. Hammer. 1988. The reaction limited kinetics of membrane to surface adhesion and detachment. *Proc. R. Soc. B.* 234:55–83.
- Dong, C., R. Skalak, K.-L.P. Sung, G. W. Schmid-Schoenbein, and S. Chien. 1988. Passive deformation analysis of human leukocytes. *J. Biomech. Eng.* 110:27–36.
- Dustin, M. L., and T. A. Springer. 1989. T-cell receptor cross-linking transiently stimulates adhesiveness through LFA-1. *Nature (Lond.)*. 341:619–624.
- Dustin, M. L., D. Olive, and T. A. Springer. 1989. Correlation of CD2 binding and functional properties of multimeric and monomeric lymphocyte function associated antigen-3. *J. Exp. Med.* 169:503–517.
- Evans, E., and A. Leung. 1984. Adhesivity and rigidity of erythrocyte membrane in relation to wheat germ agglutinin in binding. *J. Cell Biol.* 98:1201–1208.
- Evans, E., and A. Yeung. 1989. Apparent viscosity and cortical tension of blood granulocytes determined by micropipette aspiration. *Biophys. J.* 56:151–160.
- Gent, A. N. 1982. The strength of adhesive bonds. An examination of interfacial chemistry, rheology of materials, and fracture mechanics. *Adhesives Age.* 25:27–31.
- Johnson, K. L. 1985. Contact Mechanics. Cambridge Press, New York. 452 pp.
- Kalina, M., and G. Berk. 1976. Contact regions of cytotoxic T lymphocyte-target cell conjugates. *Cell Immunol.* 25:41–51.
- Kupfer, A., and S. J. Singer. 1989a. The specific interaction of helper T cells and antigen presenting B cells. Membrane and cytoskeletal reorganizations in the bound T cell as a function of antigen dose. *J. Exp. Med.* 170:1697–1713.
- Kupfer, A., and S. J. Singer. 1989b. Cell biology of cytotoxic and helper T cell functions: immunofluorescence microscopic studies of single cells and cell couples. *Annu. Rev. Immunol.* 7:309–337.
- Lawrence, M. B., and T. A. Springer. 1991. Leukocytes roll on a selectin at physiologic flow rates: distinction from and prerequisite for adhesion through integrins. *Cell.* 65:1–20.
- Marlin, S. D., and T. A. Springer. 1987. Purified intercellular adhesion molecule-1 (ICAM-1) is a ligand for lymphocyte function associated antigen-1 (LFA-1). *Cell.* 51:813–823.
- McConnell, H. M., T. H. Watts, R. M. Weiss, and A. A. Brian. 1986. Supported planar membranes in studies of cell-cell recognition in the immune system. *Biochim. Biophys. Acta.* 864:95–106.
- Meuer, S. C., O. Acuto, T. Hercend, S. F. Schlossman, and E. L. Reinherz. 1984. The human T cell receptor. *Annu. Rev. Immunol.* 2:23–50.
- Phatak, P. D., C. H. Packman, and M. A. Lichtman. 1988. Protein kinase C modulates actin conformation in human T lymphocytes. *J. Immunol.* 141:2929–2934.
- Sanders, M. E., M. W. Makgoba, S. O. Sharrow, D. Stephany, T. A. Springer, H. A. Young, and S. Shaw. 1988. Human memory T lymphocytes express increased levels of three adhesion molecules (LFA-3, CD3, LFA-1) and three other molecules (UCHL1, CDw29, and Pgp-1) and have enhanced gamma interferon production. *J. Immunol.* 140:1401–1407.
- Sanders, V. M., J. M. Snyder, J. W. Uhr, and E. S. Vitetta. 1986.

- Characterization of the physical interaction between antigen-specific B and T cells. *J. Immunol.* 137:2395–2404.
- Schmid-Schönbein, G. W. 1990. Leukocyte biophysics. *Cell Biophys.* 107–135.
- Schmidt, R. E., J. P. Caufield, J. Michon, A. Hein, M. M. Kamada, R. P. MacDermott, R. L. Stevens, and J. Ritz. 1988. T11/CD2 activation of cloned human natural killer cells results in increased conjugate formation and exocytosis of cytolytic granules. *J. Immunol.* 140:991–1002.
- Southwick, F. S., G. A. Dabiri, M. Paschetto, and S. H. Zigmond. 1989. Polymorphonuclear leukocyte adherence induces actin polymerization by a transductional pathway which differs from that used by chemoattractants. *J. Cell Biol.* 109:1561–1569.
- Springer, T. A. 1990. Adhesion receptors of the immune system. *Nature (Lond.)*. 346:425–434.
- Sung, K. L. P., L. A. Sung, M. Crimmins, S. J. Burakof, and S. Chien. 1986. Determination of junction acidity of cytotoxic T-cell and target cell. *Science (Wash. DC)*. 234:1605–1608.
- Sung, K. L. P., L. A. Sung, M. Crimmins, S. J. Burakof, and S. Chien. 1988. Dynamic changes in the viscoelastic properties in cytotoxic T lymphocyte mediated killing. *J. Cell Sci.* 91:179–189.
- Timoshenko, S. 1940. Theory of Plates and Shells. McGraw-Hill, New York. 580 pp.
- Tözeren, A. 1990. Cell-cell, cell-substrate adhesion: theoretical and experimental considerations. *J. Biomech. Eng.* 112:311–318.
- Tözeren, A., K. L. P. Sung, and S. Chien. 1989. Theoretical and experimental studies on crossbridge migration during cell disaggregation. *Biophys. J.* 55:479–487.
- Tözeren, A., K. L. P. Sung, L. A. Sung, M. L. Dustin, P. Y. Chan, T. A. Springer, and S. Chien. 1992. Micromanipulation of adhesion of a Jurkat cell to a planar membrane containing LFA-3 molecules. *J. Cell Biol.* 116:997–1006.
- Watts, T. H., A. A. Brian, J. W. Kappler, and P. Marrack. 1984. Antigen presentation by supported planar membrane containing affinity-purified I-A^d. *Proc. Natl. Acad. Sci. USA.* 81:7564–7568.
- Yeung, A., and E. Evans. 1989. Cortical shell-liquid core model for passive flow of liquid-like spherical cells into micropipets. *Biophys. J.* 56:139–149.